



5-Aminosalicylic acid ameliorates dextran sulfate sodium-induced colitis in mice by modulating gut microbiota and bile acid metabolism

Ling Huang^{1,2} · Junping Zheng¹ · Guangjun Sun¹ · Huabing Yang² · Xiongjie Sun² · Xiaowei Yao² · Aizhen Lin² · Hongtao Liu¹

Received: 28 April 2022 / Revised: 27 June 2022 / Accepted: 4 July 2022 / Published online: 1 August 2022
© The Author(s), under exclusive licence to Springer Nature Switzerland AG 2022

Abstract

Colitis develops via the convergence of environmental, microbial, immunological, and genetic factors. The medicine 5-aminosalicylic acid (5-ASA) is widely used in clinical practice for colitis (especially ulcerative colitis) treatment. However, the significance of gut microbiota in the protective effect of 5-ASA on colitis has not been explored. Using a dextran sulfate sodium (DSS)-induced colitis mouse model, we found that 5-ASA ameliorated colitis symptoms in DSS-treated mice, accompanied by increased body weight gain and colon length, and a decrease in disease activity index (DAI) score and spleen index. Also, 5-ASA alleviated DSS-induced damage to colonic tissues, as indicated by suppressed inflammation and decreased tight junction, mucin, and water–sodium transport protein levels. Moreover, the 16S rDNA gene sequencing results illustrated that 5-ASA reshaped the disordered gut microbiota community structure in DSS-treated mice by promoting the abundance of *Bifidobacterium*, *Lachnoclostridium*, and *Anaerotruncus*, and reducing the content of *Alloprevotella* and *Desulfovibrio*. Furthermore, 5-ASA improved the abnormal metabolism of bile acids (BAs) by regulating the Farnesoid X receptor (FXR) and Takeda G-protein-coupled receptor 5 (TGR5) signaling pathways in DSS-treated mice. In contrast, 5-ASA did not prevent the occurrence of colitis in mice with gut microbiota depletion, confirming the essential role of gut microbiota in colitis treatment by 5-ASA. In conclusion, 5-ASA can ameliorate DSS-induced colitis in mice by modulating gut microbiota and bile acid metabolism. These findings documented the new therapeutic mechanisms of 5-ASA in clinical colitis treatment.

Keywords 5-Aminosalicylic acid · Ulcerative colitis · Bile acid · Enterohepatic circulation · Gut microbiota

Abbreviations

Abx	Antibiotics mixture
AQPs	Aquaporins
ASBT	Apical sodium-dependent bile acid transporter
BA	Bile acid
BSH	Bile salt hydrolase
DSS	Dextran sulfate sodium

DAI	Disease activity index
ENaC	Epithelial sodium channel
FGF15	Fibroblast growth factor 15
FXR	Farnesoid X receptor
NF-κB	Nuclear factor-kappa B
NLRP3	NOD-like receptor pyrin domain containing 3
Nrf2	Nuclear erythroid 2-related factor 2
SCFAs	Short-chain fatty acids
TGR5	Takeda G protein-coupled receptor 5
UC	Ulcerative colitis
5-ASA	5-Aminosalicylic acid

Ling Huang and Junping Zheng have contributed equally to this work.

✉ Aizhen Lin
linaizhen2003@163.com

✉ Hongtao Liu
hongtaoliu@hbtcm.edu.cn

¹ College of Basic Medical Sciences, Hubei University of Chinese Medicine, Wuhan 430065, People's Republic of China

² China Hubei Provincial Hospital of Traditional Chinese Medicine, Wuhan 430061, People's Republic of China

Introduction

Inflammatory bowel diseases have brought about severe economic and medical stress [1]. Ulcerative colitis (UC) is a typical inflammatory bowel disease, and the incidence and prevalence of UC have been rising worldwide in recent years [2]. Various factors can induce UC, including genetic

variation, excessive pro-inflammatory cytokines, gut barrier dysfunction, and environmental factors [3].

In recent years, the gut microbiota has been proved to play an essential role in the pathogenesis of colitis [4]. Researchers found that gut microbiota dysbiosis is a driving force in UC development. Clinically, UC patients had decreased abundances of Firmicutes and Actinobacteria phyla and increased contents of Proteobacteria and Bacteroidetes phyla [5, 6]. Usually, the imbalanced intestinal flora will lead to metabolic dysfunction and immune disorders, as reflected by profiles of bacterial metabolites. Among them, bile acids (BAs), short-chain fatty acids (SCFAs), and tryptophan metabolites are three types of the most affected intestinal metabolites [7]. BAs are bi-directionally regulatory molecules connecting intestinal microbiota and hosts [8]. In colitis, intestinal barrier damage reduces the enterohepatic circulation of BAs and affects the BA transformation, further worsening UC symptoms [9, 10]. SCFAs (like acetic acid, propionic acid, and butyric acid) are fermented products transformed by intestinal bacteria from various carbohydrates [11]. In the intestine, SCFAs provide energy resources for colonic cells and maintain intestinal immune homeostasis [12]. The reduced abundance of butyrate-producing bacteria (e.g., *Clostridium perfringens*) was observed in UC patients, accompanied by a decreased butyric acid level [6]. In a clinical experiment, the serum levels of tryptophan metabolites had a negative correlation with the disease activity [13]. Thus, maintaining a healthy gut microbiota community should be beneficial to preventing or attenuating UC occurrence.

As a recommended drug for UC treatment by the American College of Gastroenterology [14], 5-aminosalicylic acid (5-ASA) is a hydrogen peroxide scavenger with the ability to inhibit neutrophil chemotaxis and scavenge reactive oxygen species [15, 16]. Meanwhile, 5-ASA can attenuate colitis by inducing T lymphocyte apoptosis and modulating inflammatory mediators [17]. In the previous studies, 5-ASA acted on intestinal mucosa by activating peroxisome proliferator-activated receptors γ or blocking the nuclear factor-kappa B (NF- κ B) pathway [18–20]. Furthermore, 5-ASA could change the intestinal bacteria structure in UC patients [21]. However, it remains unknown whether gut microbiota is necessary for the 5-ASA-mediated treatment of colitis.

Based on the clinical use of 5-ASA [22], we designed the experiment by oral administration of 5-ASA ($100 \text{ mg kg}^{-1} \text{ day}^{-1}$) to mice with a dextran sulfate sodium (DSS)-induced colitis and a germ-depletion experiment to examine the impact of 5-ASA on the intestinal flora, bacterial metabolites, and potential signaling pathways. In summary, this study aimed to explore how the gut microbiota was involved in the colitis treatment by 5-ASA and provide new theoretical support and ideas for further treatment of colitis using 5-ASA.

Materials and methods

Reagents

Dextran sulfate sodium (DSS, MW: 36–50 kDa) was purchased from MP Biochemicals (Santa Ana, CA, USA). 5-Aminosalicylic acid (5-ASA) was bought from MP Biochemicals (Santa Ana, CA, USA). The primary antibodies of anti- β -Actin, anti-phosphorylation-ERK, and anti-ERK were purchased from Santa Cruz Biotechnology (Santa Cruz, CA, USA). Antibodies of anti-phosphorylation-JNK, anti-JNK, anti-IL-1 β , and anti-NLRP3 (NOD-like receptor pyrin domain containing 3) were manufactured by Cell Signaling Technology (Danvers, MA, USA). Antibodies of anti-FGFR4 and anti-TGR5 were provided by Abcam (Cambridge, MA, USA). Antibodies of anti-FXR, anti-ASBT, and anti-ZO-1 were purchased from ABClonal Technology (Wuhan, China). Cholic acid (CA), deoxycholic acid (DCA), ursodeoxycholic acid (UDCA), and tauroursodeoxycholic acid (TUDCA) were provided by Sigma-Aldrich (St. Louis, MO, USA). Tauro- α -murocholic acid (T α MCA) and Tauro- β -murocholic acid (T β MCA) were obtained from TRC (Toronto, Canada). Tryptamine and indole were bought from Sigma-Aldrich (St. Louis, MO, USA). Acetate, propionate, butyrate, and pentanoic acid were purchased from Aladdin (Shanghai, China). All other chemicals were of the highest grade available.

Animal experiment

Male BALB/c mice (6-week-old, 18–22 g) were purchased from the Hubei Provincial Center for Disease Control and Prevention (Wuhan, China). All mice were housed in a temperature-controlled environment ($23 \pm 2 \text{ }^\circ\text{C}$) under a 12-h light–dark cycle with food and water ad libitum. After 1 week of adaptive feeding, the mice were randomly divided into four groups ($n = 8$): Ctrl group, DSS group, 5-ASA group, and DSS + 5-ASA group. Mice drank sterilized water with 3% DSS solution (DSS group and DSS + 5-ASA group) or without (Ctrl group and 5-ASA group) for 1 week. Meanwhile, mice in the 5-ASA group and DSS + 5-ASA group were intragastrically treated with 5-ASA ($100 \text{ mg}\cdot\text{kg}^{-1}\cdot\text{day}^{-1}$, dissolved in 2% cyclodextrin) during the week, and mice in both the Ctrl group and the DSS group were given vehicle solution (2% cyclodextrin) by gavage. After the treatment, mice were euthanized by ethyl ether, and the major tissues were collected and kept at $-80 \text{ }^\circ\text{C}$ for further analysis.

For the antibiotic treatment, male BALB/c mice were separated into four groups ($n = 8$): Ctrl group, DSS group,

DSS + Abx group, and DSS + 5-ASA + Abx group. In brief, mice in the DSS + Abx group and DSS + 5-ASA + Abx group were treated with an antibiotic mixture (Abx) (0.5 mg ml⁻¹ vancomycin, 0.5 mg ml⁻¹ metronidazole, 1 mg ml⁻¹ neomycin sulfate, and 1 mg ml⁻¹ ampicillin, dissolved in drinking water) for 2 weeks. Then, all mice were separately given sterilized water (Ctrl group), water supplemented with 3% DSS (DSS group), DSS and Abx (DSS + Abx group), or DSS and Abx and 5-ASA (100 mg kg⁻¹ day⁻¹, dissolved in 2% cyclodextrin) (DSS + 5-ASA + Abx group) for another 1 week. After the treatment, all mice were euthanized, and the major tissues were collected, as mentioned above.

All experimental animal procedures were performed following the NIH Guide for the Care and Use of Laboratory Animals and the requirement of the Ethical Experimentation Committee of Hubei University of Chinese Medicine and the National Act on Use of Experimental Animals (Permission ID: SYXK2020-0002).

Measurement of disease activity index (DAI) score and spleen index

We recorded the body weight, anal bleeding, and stool consistency of mice daily during the animal experiment. Meanwhile, we evaluated the DAI score based on the rules provided in Supplementary Methods. The body weight was recorded before sacrifice. After sacrifice, the spleen tissue of mice was collected and weighed. The spleen index was calculated according to the ratio of spleen weight to body weight.

RNA extraction and quantitative reverse transcription-polymerase chain reaction (RT-qPCR)

Total RNA was isolated from colon and liver tissues using Trizol reagents (SummerBio, Beijing, China). The isolated RNA (500 ng) was reverse transcribed into cDNA using a first-strand cDNA synthesis kit (SummerBio, Beijing, China). The RT-qPCR amplification was performed as follows: 95 °C for 10 min; 40 cycles of amplification (95 °C for 10 s, 60 °C for 30 s). The primer sequences of target genes were indicated in Supplementary Table 1, interleukin-1 β (*Il-1 β*), cyclooxygenase 2 (*Cox-2*), interleukin-6 (*Il-6*), toll-like receptor 4 (*Tlr4*), tumor necrosis factor- α (*Tnf- α*), epithelial sodium channel beta (*Enac- β*), *Enac- γ* , zonula occludens protein 1 (*Zo-1*), aquaporin 4 (*Aqp4*), *Aqp2*, Mucin 3 (*Muc-3*), Farnesoid X Receptor (*Fxr*), apical sodium-dependent bile acid transporter (*Asbt*), cholesterol 7 α -hydroxylase (*Cyp7a1*), sterol 12 α -hydroxylase (*Cyp8b1*), cytochrome sterol 27-hydroxylase (*Cyp27a1*), and glyceraldehyde-3-phosphate dehydrogenase (*Gapdh*). Each primer pair was considered specific when the melting curve displayed a

single sharp peak. All mRNA levels were normalized using *Gapdh* as an internal reference. The relative gene expression was calculated using the 2^(- $\Delta\Delta C_t$) method.

Western blot

Total proteins from colon and liver tissues were lysed and extracted with RIPA buffer (Beyotime, Shanghai, China). Samples were separated using a sodium dodecyl sulfate–polyacrylamide gel and transferred to a polyvinylidene difluoride (PVDF) membrane for separation. After blocking with 5% skim milk in TBST for 1 h, the membranes were incubated with primary antibodies overnight at 4 °C. Next, the membranes were exposed to a secondary antibody ligated with horseradish peroxidase (HRP) (Cell Signaling Technology, MA, USA) for 1 h. Finally, the protein bands were detected by enhanced chemiluminescence (ECL) (Sigma-Aldrich, MO, USA), and the band densitometry was analyzed using Image J2x software (National Institute of Health, Bethesda, MD, USA).

Histological analysis

Colon tissues were fixed with 4% paraformaldehyde, embedded in paraffin, and sectioned into 5 μ m slides. After the deparaffinization with xylene and the rehydration with gradient ethanol, slides were stained for histopathological examination using a hematoxylin and eosin (H&E) staining kit (Beyotime, Shanghai, China). The production of glycosylated mucins in colon tissues was assessed by immunofluorescence staining with fluorescein isothiocyanate conjugated-wheat germ agglutinin (WGA-FITC) (Sigma-Aldrich, St. Louis, MO, USA). The acidic mucins were detected using an Alcian blue staining kit (Vectorlabs, Beijing, China). The expressions of ZO-1 and ENaC- γ were analyzed by immunohistochemical staining. The photomicrographs were captured using a Leica DMIL microscope equipped with a DFC450C digital camera (Leica Microsystems, Wetzlar, Germany). The histological score of H&E staining was evaluated according to Supplementary Table 2 [23]. Quantification of Alcian blue and WGA-FITC staining was calculated by Image J2x software (National Institute of Health, Bethesda, MD, USA).

Quantification of intestinal metabolites in feces

To quantify the contents of BAs in feces, we homogenized 50 mg of the fecal sample with 1 mL of water–methanol–formic acid solution (25:74:1, V/V/V) containing d5-CA and d4-TCA as internal standards with a final concentration of 0.2 μ g·ml⁻¹. The standards of BAs were dissolved in methanol. To determine the contents of SCFAs, we homogenized 50 mg of the fecal sample with 1 ml of 50% (V/V)

methanol-aqueous solution (containing 0.2% HCl). To detect the contents of tryptophan catabolites, we homogenized 50 mg of the fecal sample with 1 ml of pre-cooled methanol. After the homogenization using a KZ-II grinding machine (Servicebio, Wuhan, China), the fecal mixtures were centrifuged at $12,000\times g$ for 15 min at 4 °C. Then, the supernatant was collected and filtered through a 0.22 μm aqueous or organic membrane. After that, all samples were used for gas chromatography–mass spectrometry (GC–MS) or liquid chromatography–mass spectrometry (LC–MS) analysis. The detailed analytical conditions were provided in Supplementary Methods.

16S rDNA gene sequencing

Genomic DNA from fecal samples was extracted following the protocol of Fast DNA™ SPIN Kit (MP Biomedicals, CA, USA), which was used for amplification of the V3–V4 hypervariable region of the 16S rDNA gene. The sequencing of 16S rDNA gene amplicon was performed on an Illumina MiSeq platform (Illumina, San Diego, CA, USA) by Beijing Allwegene Tech, Ltd (Beijing, China). The detailed information about library construction, bacterial abundance analysis, and functional prediction of fecal samples was described in the Supplementary Methods.

Statistical analysis

GraphPad Prism 8.2 software (La Jolla, CA, USA) was adopted for statistical analysis. Data were presented as mean \pm standard deviation. Differences among groups were analyzed by a two-way analysis of variance (ANOVA) followed by the Bonferroni post hoc test. For all statistical tests, $P < 0.05$ was considered significance.

Results

5-ASA relieves symptoms of colitis in DSS-treated mice

We first assessed whether 5-ASA relieved symptoms of colitis in DSS-treated mice. As indicated in Fig. 1a and Supplementary Fig. 1a, we observed a continuous loss of body weight in DSS-treated mice ($P < 0.01$, vs. Ctrl group), but 5-ASA inhibited this downward trend ($P < 0.01$, vs. DSS group). After DSS treatment for 5 days, the DSS-treated mice exhibited typical symptoms of colitis, including diarrhea, hematochezia, and weight loss, which were displayed by the higher disease activity index (DAI) score ($P < 0.05$ or $P < 0.01$, vs. Ctrl group) (Fig. 1b and Supplementary Fig. 1b). In contrast, the DAI score of mice in the DSS + 5-ASA group was distinctly decreased compared

to the DSS group ($P < 0.01$) (Fig. 1b and Supplementary Fig. 1b). Also, 5-ASA suppressed the shortening of colon length and the increase of spleen index ($P < 0.05$ or $P < 0.01$, vs. DSS group) (Fig. 1c–e). The histochemical results indicate that 5-ASA alleviated damage to the villous membrane and increased the thickness of muscle layers in colon tissues of DSS-treated mice (Fig. 1f), as was evidenced by the restored histopathological score ($P < 0.01$, vs. DSS group). The WGA-FITC and Alcian blue staining suggest that 5-ASA partly lessened the destruction of glycosylated and acidic colonic mucins in DSS-treated mice ($P < 0.01$, vs. DSS group) (Fig. 1g and h). From the above results, 5-ASA significantly improved the colitis-related symptoms in DSS-treated mice.

5-ASA restrains colonic inflammation and gut barrier impairment in DSS-treated mice

Next, we assessed the inhibitory effect of 5-ASA on colonic inflammation and gut barrier integrity in DSS-treated colitis mice. By RT-qPCR analysis, we found that the mRNA levels of *Il-1 β* , *Cox-2*, *Il-6*, *Mcp-1*, and *Tlr4* were higher in colon tissues of DSS-treated mice than those of the Ctrl group ($P < 0.05$) (Fig. 2a). On the contrary, 5-ASA suppressed the transcription of these pro-inflammatory cytokines ($P < 0.05$, vs. DSS group) (Fig. 2a). To investigate which signal pathways regulated the above inflammatory indicators, we examined the mitogen-activated protein kinases (MAPKs) and NLRP3, both of which were found to be responsible for the occurrence of colitis [24]. Though 5-ASA failed to inhibit the changes of p38 and ERK1/2 MAPKs in colon tissues of DSS-induced colitis (Data not shown), it statistically reversed the upregulations of NLRP3, IL-1 β , and p-JNK at protein levels (Fig. 2b and c). Diarrhea is another typical colitis symptom, associated with the imbalanced transportations of electrolytes and water fluid [25]. As shown in Fig. 2d, 5-ASA blocked the mRNA reductions of water–sodium transport-related mediators in colon tissues of DSS-treated mice, including *Enac- β* , *Enac- γ* , *Aqp2*, and *Aqp4* ($P < 0.05$, vs. DSS group). Also, 5-ASA partly attenuated DSS-induced disruption of gut barrier integrity, as indicated by the increments of tight-junction proteins and mucoproteins at mRNA levels in DSS-treated mice, such as *Zo-1* ($P < 0.05$, vs. DSS group) and *Muc-3* (Fig. 2e). Immunohistochemical staining of ZO-1 and ENaC- γ confirmed the improvement of 5-ASA on gut barrier destruction and water–electrolyte disturbance in DSS-treated mice (Fig. 2f and g). By WB analysis, 5-ASA up-regulated the protein expression of ZO-1 in DSS-treated mice (Supplementary Fig. 1c). The results demonstrated that 5-ASA ameliorated the colonic inflammation and gut barrier damage in DSS-induced colitis.

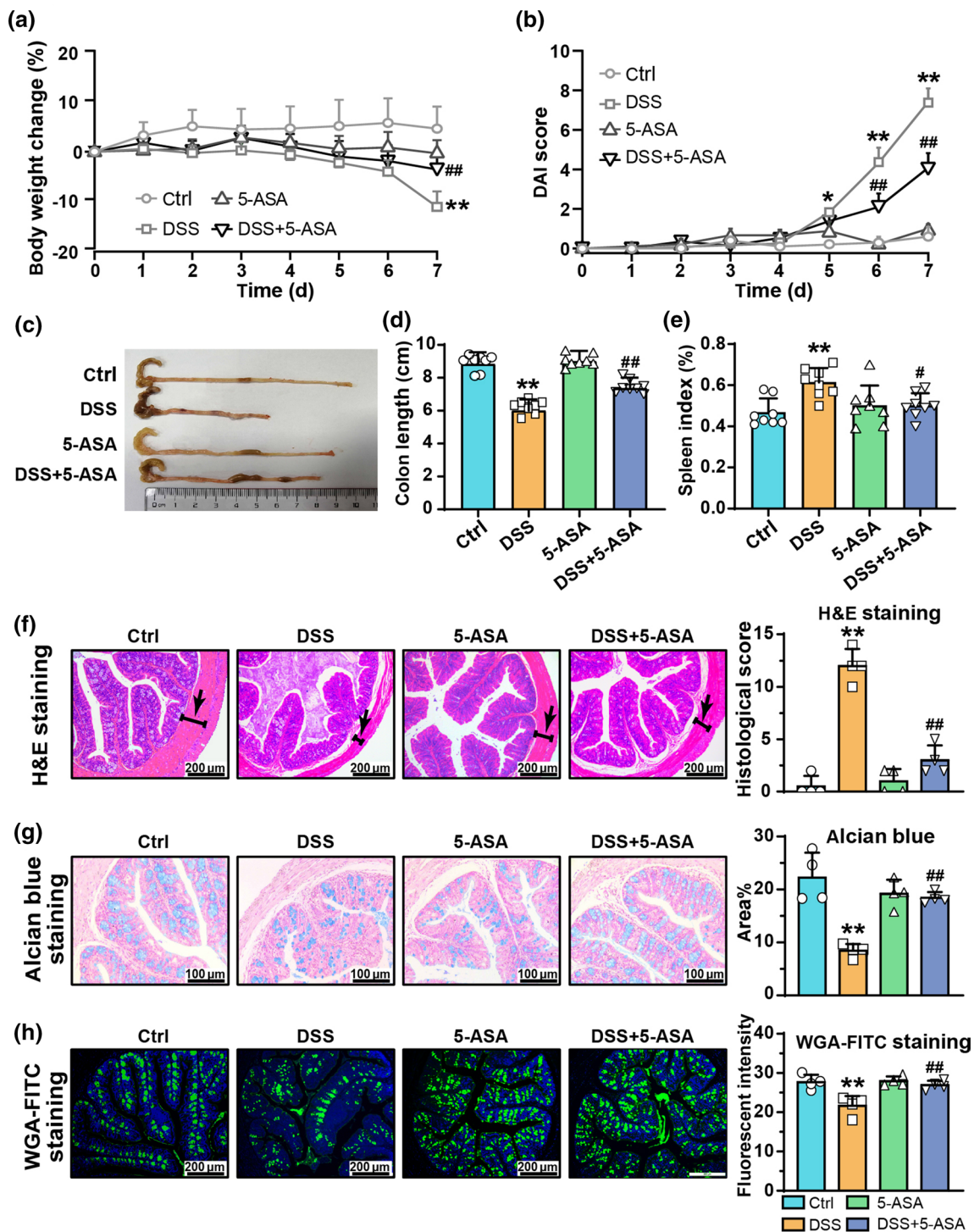


Fig. 1 Effect of 5-ASA on pathological symptoms of DSS-induced colitis. DSS-treated BALB/c mice were intragastrically administered with 5-ASA ($100 \text{ mg} \cdot \text{kg}^{-1} \cdot \text{day}^{-1}$) for 1 week. **a** Body weight gain. **b** Disease activity index score. **c–e** Colon photograph (**c**), Colon length (**d**), and Spleen index (**e**) of mice among four experimental groups. **f–h** Morphological analysis of colonic tissues by hematoxylin & eosin (H&E) staining (**f**) (scale bar = $200 \mu\text{m}$, magnification of the microphotograph, $\times 200$), Alcian blue staining (**g**) (scale

bar = $100 \mu\text{m}$, magnification of the microphotograph, $\times 200$), and Wheat germ agglutinin labeled with FITC (WGA-FITC) staining (**h**) (scale bar = $200 \mu\text{m}$, magnification of the microphotograph, $\times 100$). Black arrow indicates a muscular layer. Quantification of Alcian blue and WGA-FITC staining by Image J2x software. DAI disease activity index. Data were represented as mean \pm SD ($n = 8$). * $P < 0.05$, ** $P < 0.01$, vs. Ctrl group; # $P < 0.05$, ## $P < 0.01$, vs. DSS group

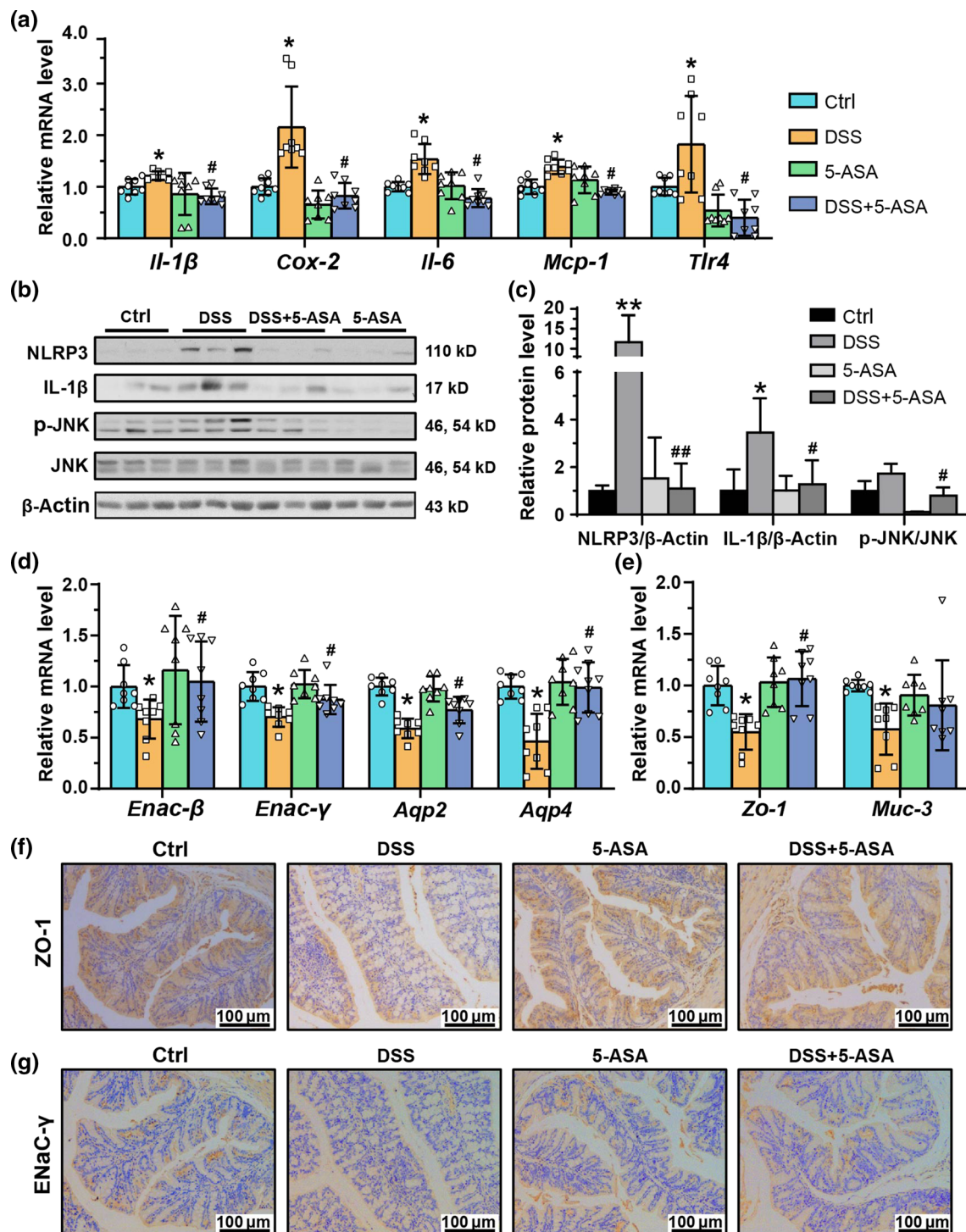


Fig. 2 Inhibition of 5-ASA administration on colonic inflammation and structural destruction in DSS-induced mice. DSS-treated BALB/c mice were intragastrically administered with 5-ASA ($100 \text{ mg} \cdot \text{kg}^{-1} \cdot \text{day}^{-1}$) for 1 week. After the treatment, all mice were euthanized, and colon tissues were collected for further analysis. **a** The mRNA expressions of intestinal inflammation-related indicators were analyzed by RT-qPCR. **b** Protein levels of NLRP3, IL-1 β , p-JNK, and

JNK were assayed by Western blot. **c** Quantification of band intensity using Image J2x software. **d**, **e** Expression of water-sodium transport and gut barrier in colon tissues at mRNA level by qRT-PCR. **f**, **g** Immunohistochemical analysis of ZO-1 (**f**) and ENaC- γ (**g**) in colon tissues (scale bar = 100 μm , magnification of the microphotograph, $\times 200$). Data were presented as mean \pm SD ($n = 8$). * $P < 0.05$, ** $P < 0.01$, vs. Ctrl group; # $P < 0.05$, ### $P < 0.01$, vs. DSS group

5-ASA improves gut microbiota structure in DSS-treated mice

To investigate the effect of 5-ASA administration on the gut microbiota community of DSS-treated mice, we characterized the gut microbiota structures of 32 samples among four experimental groups based on V3–V4 variable regions by 16S rDNA gene sequencing. As shown in Supplementary Table 3, we obtained 2,862,967 sequencing reads in total. After removing 85,456 low-quality reads, 2,777,511 remained, clustered in 1497 operational taxonomic units (OTU) with similarities above 97%. Then, we evaluated species diversity within microbiome samples by PD whole tree, Shannon index, Observed species, and Chao1 index. There was no statistical significance among four experimental groups (Fig. 3a and Supplementary Fig. 2a–c). However, four distinct clusters were on the Partial Least Squares Discriminant Analysis (PLS-DA) plot, indicating the different microbial structures among four experimental groups (Fig. 3b).

Next, we analyzed the relative abundances of gut microbiota among four experimental groups. At phylum levels, we detected the decreased contents of Firmicutes and elevated abundances of Bacteroidetes and Proteobacteria in DSS-treated mice, which failed to be reversed by 5-ASA treatment (Fig. 3c and Supplementary Fig. 2d). At family levels, 5-ASA remarkably reduced Desulfovibrionaceae and Lactobacillaceae abundances, but increased the contents of Ruminococcaceae, Bacteroidaceae, and Bacteroidales S24-7 group in DSS-treated mice (Fig. 3d). Next, we screened 28 genera with the most changed abundances based on heatmap analysis among the experimental group. As suggested in Fig. 3e, we detected the changed abundances of the DSS group's bacteria. Some of them were up-regulated, such as *Alloprevotella*, *Coprococcus 1*, *Escherichia-Shigella*, *Enterorhabdus*, and *Desulfovibrio*. And the others were down-regulated, like *Lachnospirillum*, *Roseburia*, and *Anaerotruncus*. In contrast, 5-ASA treatment restored most of them to normal levels. And the levels of *Bifidobacterium* and *Romboutsia* in colitis mice were increased only in the DSS + 5-ASA group.

We used linear discriminant analysis effect size (LEfSe) to identify the characteristic bacterial taxa among four experimental groups. As revealed in Fig. 4a, one bacterial taxon in the Ctrl group was different from those of the other three experimental groups. The specific taxa numbers in the DSS group, 5-ASA group, and DSS + 5-ASA group were seven, nine, and nine. Furthermore, we conducted linear discriminant analysis (LDA) to identify the bacterial taxa with the most remarkable abundance differences (Fig. 4b): (1) *g_Lachnospirillum*, *g_Anaerotruncus*, *s_mouse_gut_metagenome*, *g_mouse_gut_metagenome*, and *g_Eubacterium_xylanophilum* for the Ctrl group;

(2) *g_Odoribacter*, *g_Desulfovibrio*, *f_Desulfovibrionaceae*, *o_Desulfovibrionales*, and *c_Deltaproteobacteria* for the DSS group; (3) *p_Firmicutes*, *f_Lachnospiraceae*, *c_Clostridia*, *o_Clostridiales*, and *g_Roseburia* for the 5-ASA group; (4) *p_Bacteroides*, *c_Bacteroidia*, *o_Bacteroidales*, *g_Bacteroides*, and *f_Bacteroidaceae* for the DSS + 5-ASA group. The above results indicated that 5-ASA partly reversed gut microbiota dysbiosis in DSS-treated mice.

5-ASA affects the production of intestinal metabolites in DSS-treated mice

To investigate the effect of 5-ASA administration on metabolite production in the intestinal tract of DSS-treated mice, we detected the levels of BAs, SCFAs, and tryptophan catabolites in fecal samples by LC–MS or GC–MS. As indicated in Fig. 5a and b, 5-ASA remarkably decreased the total BAs and primary BAs but increased the secondary BAs in feces of DSS-treated mice ($P < 0.05$ or $P < 0.01$, vs. DSS group). Then, we quantified the fecal contents of individual BAs in mice of each group. Among these BAs, the productions of CA, α MCA, and β MCA were increased, whereas the levels of TUDCA and UDCA were reduced in DSS-treated mice as compared to the Ctrl group ($P < 0.05$ or $P < 0.01$) (Fig. 5c). Conversely, 5-ASA statistically reversed the BA changes in DSS-treated mice ($P < 0.05$, vs. DSS group). Though the systemic decrease of SCFAs (acetic acid, propionic acid, butanoic acid, and pentanoic acid) in feces of DSS-treated mice, 5-ASA administration did not affect their production (Fig. 5d). Additionally, 5-ASA restored the decreased indole in DSS-treated mice to an average level ($P < 0.05$, vs. DSS group) (Fig. 5e). Based on the above, 5-ASA notably remodeled gut microbiota-related metabolite profiles, especially for bile acids.

5-ASA regulates BA metabolism-related mediators and signaling pathways in DSS-treated mice

To explore the regulatory effect of 5-ASA on the enterohepatic circulation of BAs in DSS-treated mice, we analyzed the expressions of BA metabolism-related mediators in the colon by RT-qPCR and Western blot. As suggested in Fig. 6a, 5-ASA elevated the mRNA levels of *Fxr*, *Fgf15*, and *Asbt* in colon tissues of DSS-treated mice ($P < 0.05$, vs. DSS group), which were decreased in the DSS group ($P < 0.05$, vs. Ctrl group). Expressions of *Tgr5* and *Ost- α* at mRNA levels had no changes among the four experimental groups (Fig. 6a). Furthermore, the attenuated protein expressions of FXR and ASBT in DSS-treated mice were reversed by 5-ASA treatment (Fig. 6b, c). However, the protein expression of TGR5 in colons was varied without significance among these four groups (Fig. 6b and c). Considering that

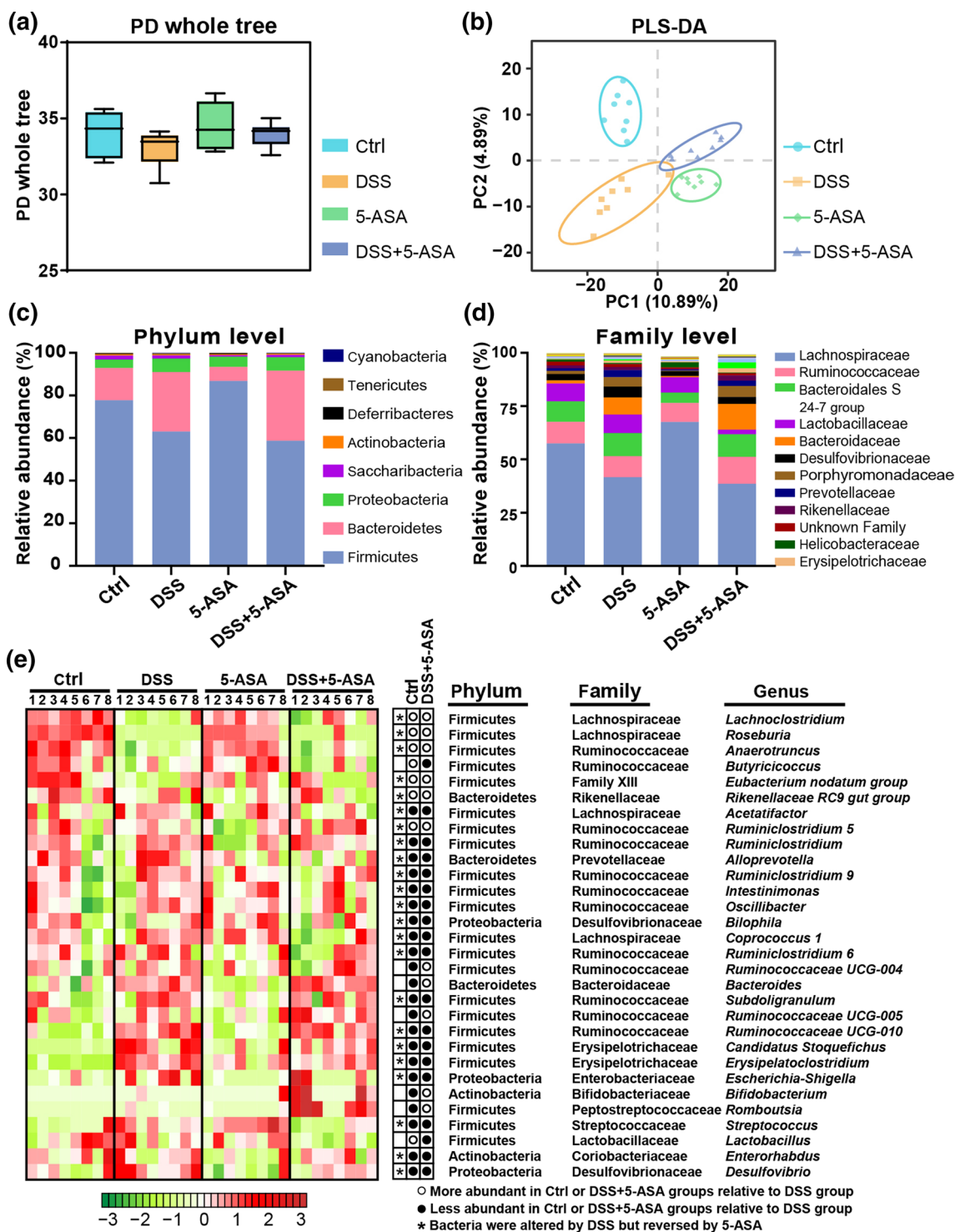


Fig. 3 Alterations in diversity and composition of gut microbiota in DSS-treated mice with 5-ASA administration. DSS-treated BALB/c mice were intragastrically administered with 5-ASA (100 mg·kg⁻¹·day⁻¹) for 1 week. After the treatment, all mice were euthanized, and fecal samples were collected for 16S rDNA gene sequencing.

a PD whole tree for α diversity. **b** Partial Least Squares Discrimination Analysis (PLS-DA) for β diversity. **c** Alteration of microbial composition at family levels. **d** Representative genera among four experimental groups. Data were presented as mean \pm SD ($n=8$)

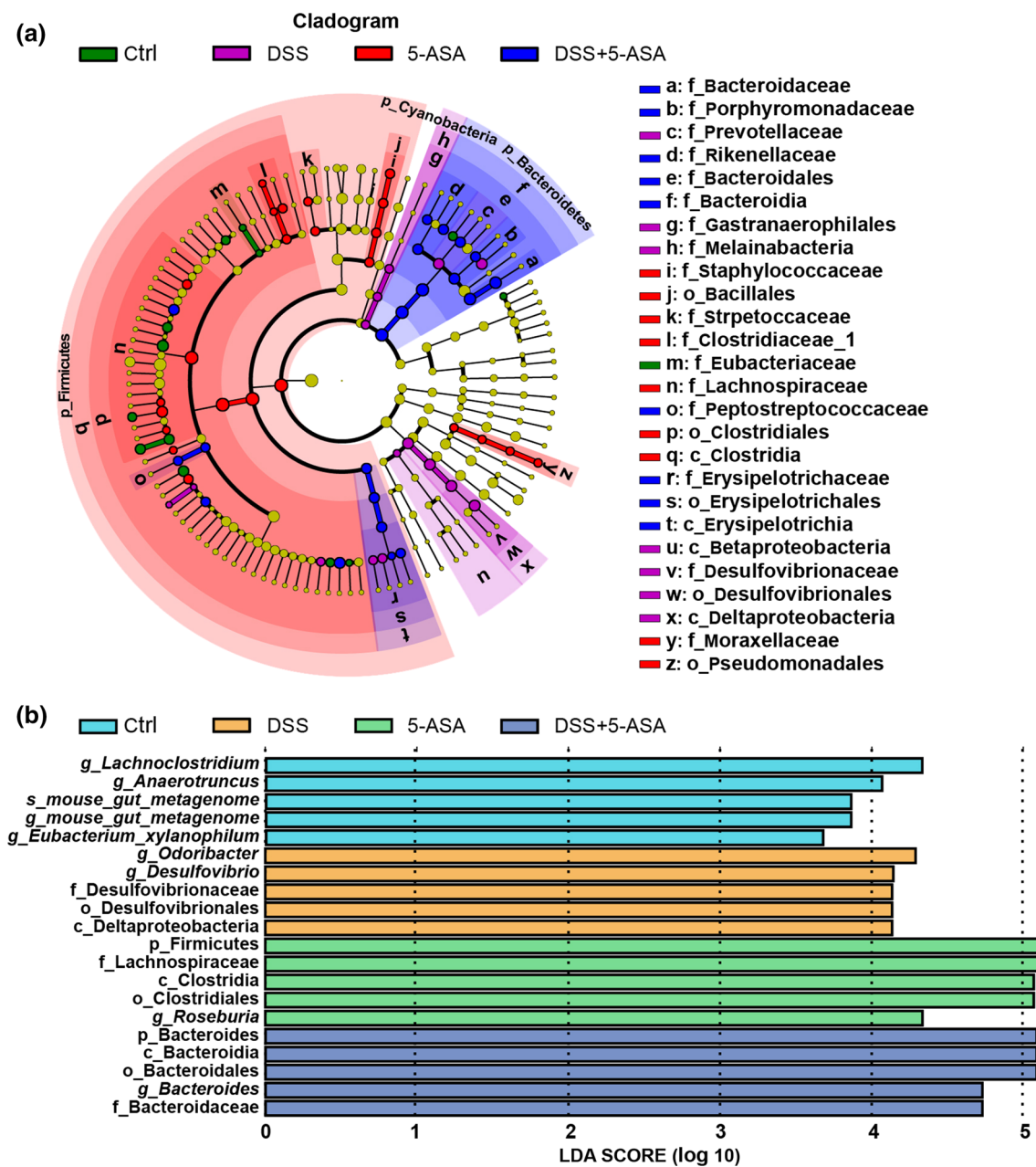


Fig. 4 Identification of characteristic taxa with the greatest difference among four experimental groups. DSS-treated BALB/c mice were intragastrically administered with 5-ASA ($100 \text{ mg}\cdot\text{kg}^{-1}\cdot\text{day}^{-1}$) for 1 week. After the treatment, all mice were euthanized, and fecal samples were collected for 16S rDNA gene sequencing. **a** Analysis

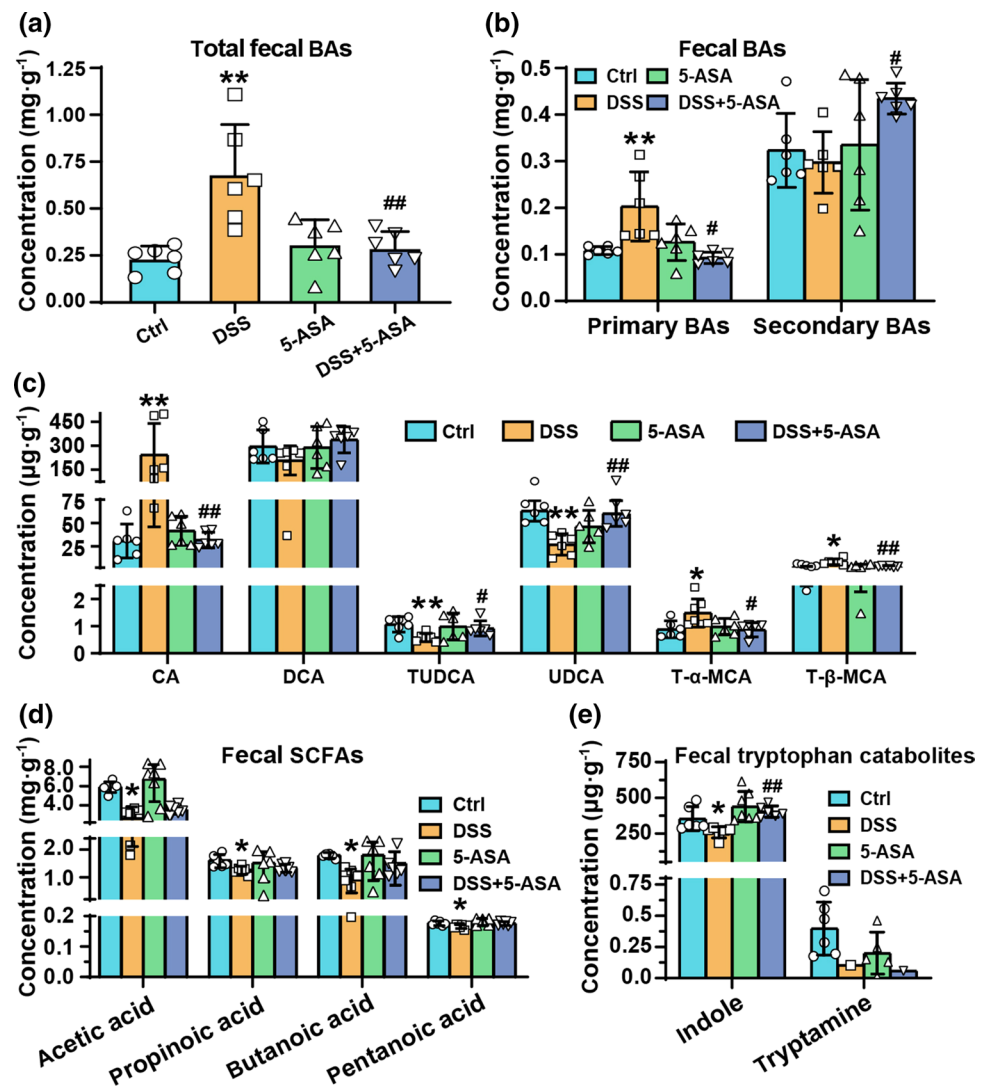
of characteristic taxa among four experimental groups by linear discriminant analysis (LDA) effect size (LEfSe). **b** Characteristic taxa using LDA with a threshold score >3.0 . Bar length of LDA represents the impact of characteristic taxa in individual groups

the reabsorption of bile acids mainly occurred in the ileum, we detected the expressions of ASBT and FXR in ileum tissues. Still, we found no changes among the four experimental groups (Data not shown).

Using RT-qPCR, we analyzed the transcriptional levels of bile acid-associated proteins and inflammatory cytokines. As shown in Fig. 7a, b, 5-ASA suppressed the hepatic expressions of BA-synthesis enzymes (*Cyp7a1*,

Cyp27a1, and *Cyp8b1*) and pro-inflammatory cytokines (*Il-1 β* and *Tnf- α*) at mRNA levels in DSS-treated mice ($P < 0.05$, vs. DSS group). However, the promoting effect on FXR was not observed in hepatic tissue of 5-ASA-treated colitis mice (Fig. 7b). Moreover, the protein levels of upstream signaling pathways responsible for BA synthesis were assayed among experimental groups. As depicted in Fig. 7c, 5-ASA reversed the over-expression

Fig. 5 Effect of 5-ASA on productions of fecal BAs, SCFAs, and tryptophan metabolites in DSS-treated mice. DSS-treated BALB/c mice were intragastrically administered with 5-ASA ($100 \text{ mg}\cdot\text{kg}^{-1}\cdot\text{day}^{-1}$) for 1 week. After the treatment, all mice were euthanized, and fecal samples were collected for LC–MC or GC–MS analyses. **a** Quantification of total BAs in feces. **b** Quantification of primary BAs and secondary BAs in feces. **c** Quantification of individual BAs in feces. **d** Quantification of SCFAs in feces. **e** Quantification of tryptophan catabolites in feces. Data were presented as mean \pm SD ($n=6$). * $P<0.05$, ** $P<0.01$, vs. Ctrl group; # $P<0.05$, ## $P<0.01$, vs. DSS group



of BA receptors (TGR5) ($P<0.01$, vs. DSS group) in the liver of DSS-treated mice. Though 5-ASA slightly elevated the protein level of fibroblast growth factor receptors (FGFR4), there was no statistically significant difference between the DSS group and the DSS + 5-ASA group ($P=0.1827$). Also, 5-ASA largely inhibited the hepatic activation of MAPKs, as indicated by the increased phosphorylation of p-JNK and p-ERK in DSS-treated mice (Fig. 7d).

To explore the association of gut microbiota with BA metabolism in DSS-treated mice, we studied the relationship between the most changed intestinal bacteria with physiological indices, individual BAs, and BA metabolism-related mediators. Spearman's correlation analysis indicated that most altered bacteria at genus levels were negatively or positively correlated with physiological indicators, BA synthesis, BA receptor (FXR), and BA

transporter (ASBT). The result suggested a vital role of gut microbiota in the occurrence of colitis (Supplementary Fig. 3).

5-ASA fails to improve colitis symptoms in DSS-treated mice with gut microbiota depletion

To confirm the pivotal role of gut microbiota in 5-ASA-initiated treatment of colitis, we treated mice with Abx to deplete the intestinal flora (Fig. 8a). Two weeks later, RT-qPCR was used to assay the concentrations of gut bacteria (Primer sequences displayed in Supplementary Table 4). The Abx almost destroyed all bacteria and individual bacteria in the intestine of mice (Supplementary Fig. 4). Compared to the DSS group, 5-ASA did not reverse the changes in DAI scores and colon length in DSS-treated mice (Fig. 8b and Supplementary Fig. 5). Moreover, 5-ASA failed to rescue

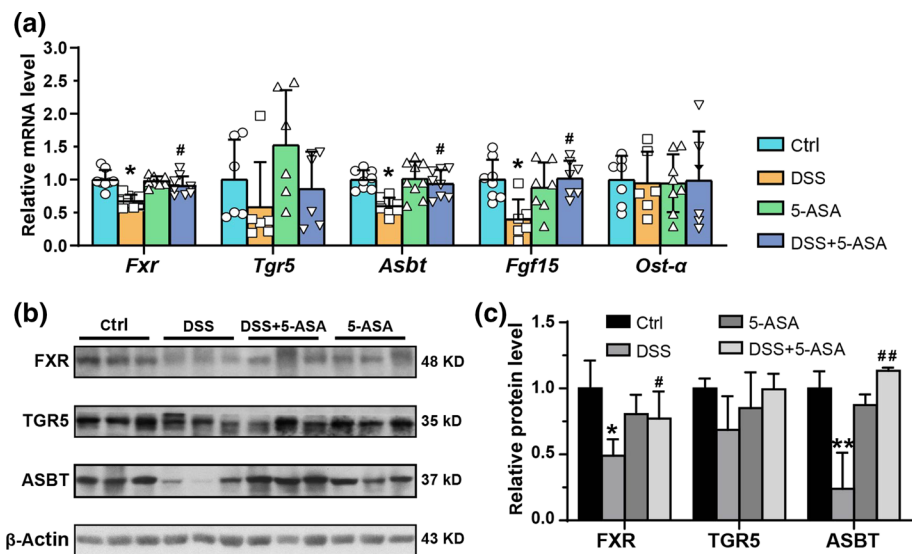
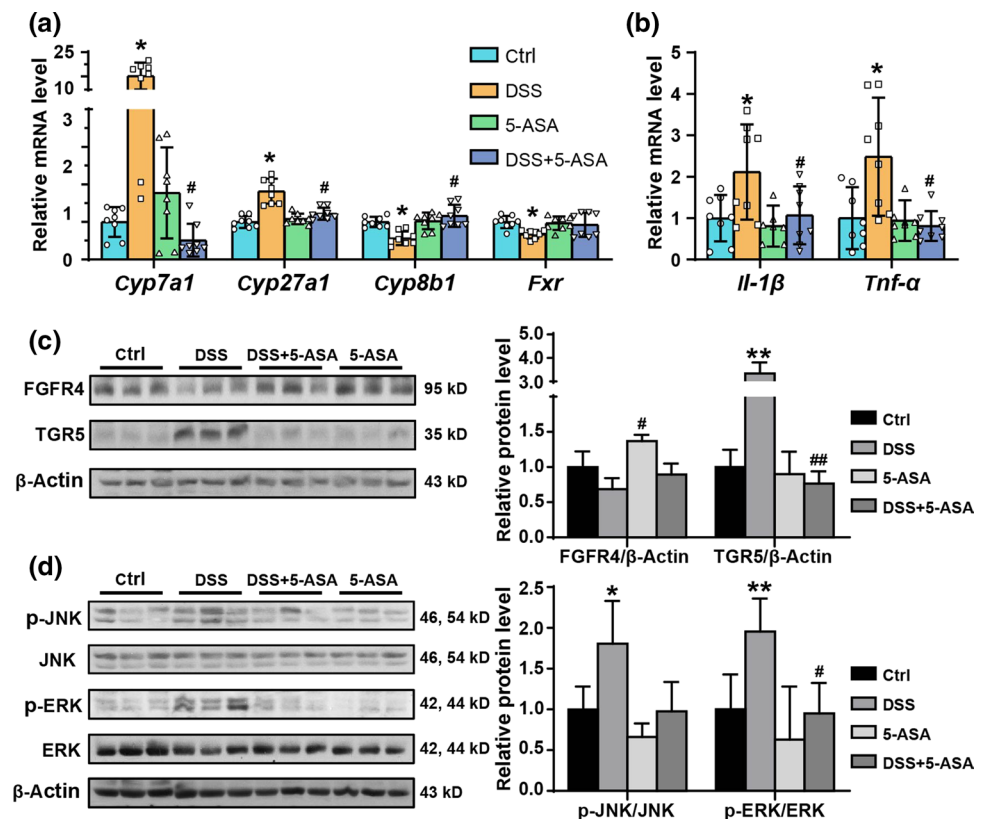


Fig. 6 Regulatory effect of 5-ASA on BA metabolism-related mediators and signaling pathways in colonic tissue of DSS-treated mice. DSS-treated BALB/c mice were intragastrically administered with 5-ASA ($100 \text{ mg}\cdot\text{kg}^{-1}\cdot\text{day}^{-1}$) for 1 week. After the treatment, all mice were euthanized, and the colon tissues were collected for further analysis. **a** Colonic mRNA levels of *Fxr*, *Tgr5*, *Asbt*, *Fgf15*, and

Ost-α were analyzed by RT-qPCR. **b** Colonic protein levels of FXR, TGR5, and ASBT were assayed by Western blot. **c** Quantification of band intensity in **b** using Image J2x software. Data were presented as mean \pm SD ($n=6-8$). * $P < 0.05$, ** $P < 0.01$, vs. Ctrl group; # $P < 0.05$, ## $P < 0.01$, vs. DSS group

Fig. 7 Regulatory effect of 5-ASA on BA metabolism-related mediators and signaling pathways in hepatic tissue of DSS-treated mice. DSS-treated BALB/c mice were intragastrically administered with 5-ASA ($100 \text{ mg}\cdot\text{kg}^{-1}\cdot\text{day}^{-1}$) for 1 week. After the treatment, all mice were euthanized, and the gut and liver tissues were collected for further analysis. **a** mRNA levels of *Fxr* and bile acid-synthesis enzymes (*Cyp7a1*, *Cyp27a1*, and *Cyp8b1*) in liver tissues. **b** mRNA levels of pro-inflammatory cytokines (*Il-1β* and *Tnf-α*) in liver tissues. **c** Protein levels of BA receptors (FGFR4 and TGR5) in liver tissues. **d** Phosphorylated levels of JNK and ERK in liver tissues. Quantification of band intensity using Image J2x software. Data were presented as mean \pm SD ($n=8$). * $P < 0.05$, ** $P < 0.01$, vs. Ctrl group; # $P < 0.05$, ## $P < 0.01$, vs. DSS group



the damage to the gut barrier structure of DSS-treated mice, such as the reduction of muscle layers and the attenuation of glycosylated and acidic colonic mucins (Fig. 8c–e).

Compared to conventional colitis mice, the gut microbiota-depleted colitis also exhibited colonic inflammation, as reflected by the elevated mRNA levels of *Il-1β*,

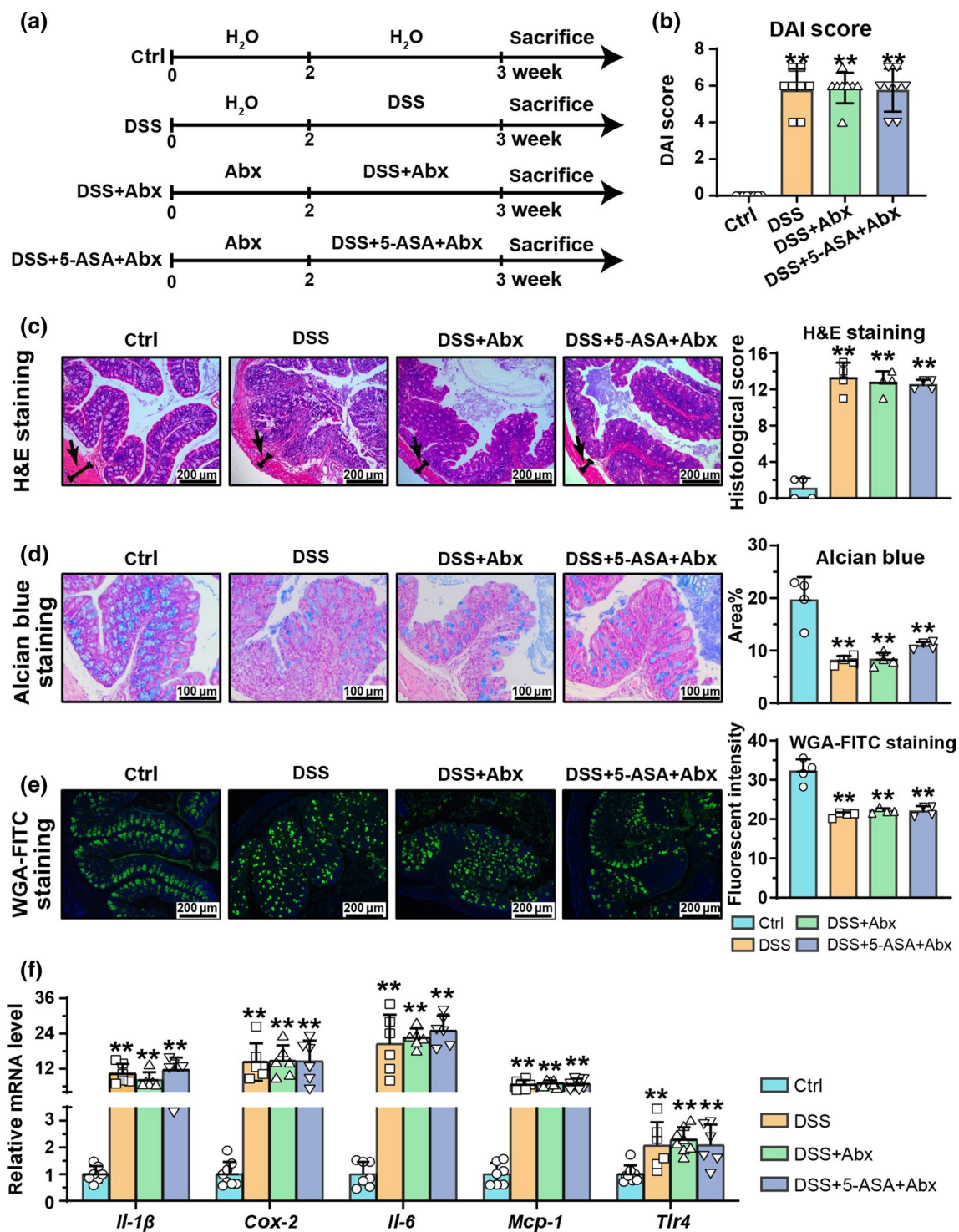


Fig. 8 Effect of 5-ASA on physiological indices and intestinal damage of DSS-treated mice with depleted gut microbiota. **a** Mice were treated with Abx (1.0 mg·ml⁻¹ ampicillin, 1.0 mg·ml⁻¹ neomycin sulfate, 0.5 mg·ml⁻¹ vancomycin, and 0.5 mg·ml⁻¹ metronidazole) for 4 weeks, followed by the administration of DSS or DSS+5-ASA. **b** Disease activity index score (DAI). **c–e** Morphological analysis of colonic tissues by hematoxylin & eosin (H&E) staining (**e**) (scale bar=200 μ m, magnification of the microphotograph, \times 100), Alcian

blue staining (**f**) (scale bar=100 μ m, magnification of the microphotograph, \times 200), and Wheat germ agglutinin labeled with FITC (WGA-FITC) staining (**g**) (scale bar=200 μ m, magnification of the microphotograph, \times 100). Black arrow indicates a muscular layer. Quantification of Alcian blue and WGA-FITC staining by Image J2x software. **f** mRNA expressions of intestinal inflammation-related mediators were analyzed by RT-qPCR. Data were presented as mean \pm SD ($n=8$). ** $P<0.01$, vs. Ctrl group

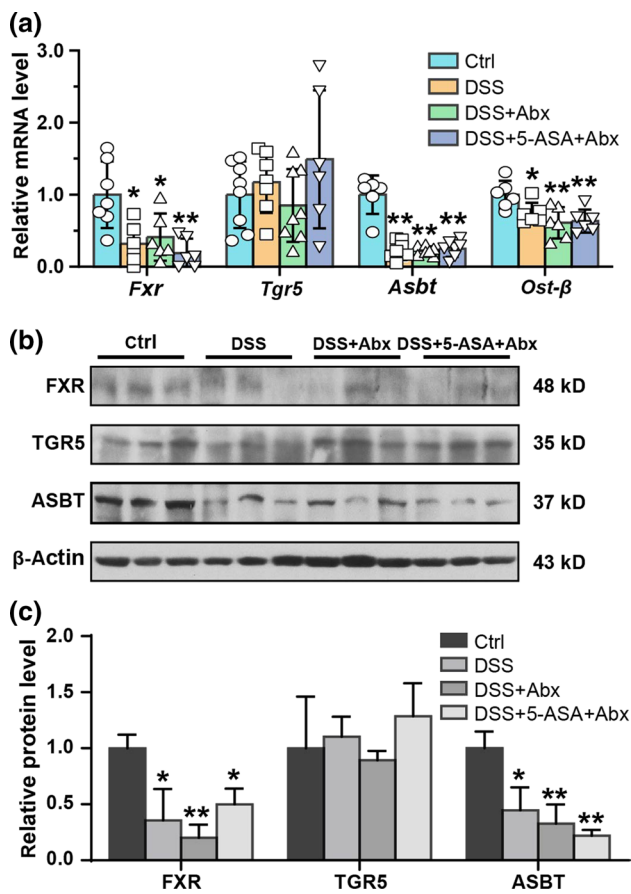


Fig. 9 Regulation of 5-ASA on BA-related mediators in colonic tissue of Abx-treated colitis mice. BALB/c mice pre-treated with Abx for two weeks were administered with DSS (3%) or 5-ASA (100 mg·kg⁻¹·day⁻¹) for 1 week. All mice were euthanized after the treatment, and the colon tissues were collected for further analysis. **a** Colonic mRNA levels of *Fxr*, *Tgr5*, *Asbt*, and *Ost-β* were analyzed by RT-qPCR. **b** Colonic protein levels of FXR, TGR5, and ASBT were assayed by Western blot. **c** Quantification of band intensity using Image J2x software. Data were presented as mean ± SD ($n=6-8$). * $P < 0.05$, ** $P < 0.01$, vs. Ctrl group

Cox-2, *Il-6*, *Mcp-1*, and *Tlr4* (Fig. 8f). Of note, the anti-inflammatory effect of 5-ASA disappeared in colon tissues of DSS-treated mice with Abx treatment (Fig. 8f). To examine the impact of gut microbiota depletion on bile acid metabolism in DSS-treated mice, we detected the BA-related regulators in colon tissues. As indicated in Fig. 9a, 5-ASA failed to reverse the changed mRNA levels of *Fxr*, *Asbt*, and *Ost-β* in germ-depleted colitis mice, and so did the protein changes of FXR and ASBT (Fig. 9b, c). Similar results were also observed in liver tissues, in which 5-ASA failed to suppress the mRNA alterations of *Cyp7a1*, *Cyp27a1*, *Cyp8b1*, *Fxr*, and *FGFR4* (Supplementary Fig. 6a, b). The mRNA and protein levels of colonic

TGR5 remained unchanged among four experimental groups (Fig. 9). The above evidence further confirmed the importance of gut microbiota and FXR-related BA metabolism in the treatment of 5-ASA on colitis.

Discussion

To date, researchers have paid great attention to the treatment of colitis for its threats to modern people's daily lives. Inspired by the critical role of gut microbiota in the pathogenesis of colitis, fecal microbial transplantation, probiotics, and prebiotics were applied to restore the destroyed intestinal flora structure of colitis patients [6]. Though 5-ASA is the first-line drug for colitis therapy, no solid evidence reveals the significance of gut microbiota in 5-ASA-initiated pharmacological effect on colitis. This study documented that 5-ASA ameliorated DSS-induced colitis in mice by regulating imbalanced gut microbiota and subsequent bile acid metabolism.

Colitis results in persistent and recurrent mucosal inflammation in the colon, and is characterized by weight loss, diarrhea, and hematochezia [26]. In this study, 5-ASA reduced the DAI score and increased the colon length in DSS-treated mice, suggesting the therapeutic effect of 5-ASA on colitis symptoms (Fig. 1a–d). Also, 5-ASA improved the spleen hypertrophy of DSS-induced colitis mice, as indicated by the decreased spleen index (Fig. 1e). It was consistent with a previous study that reported the rapid lymphocyte proliferation and size increase in the spleen of UC mice, implying that 5-ASA might reduce intestinal inflammation by affecting systemic immunity. Indeed, we observed that 5-ASA statistically down-regulated the protein level of NLRP3 and mRNA expressions of pro-inflammatory cytokines in colon tissues of DSS-treated mice (Fig. 2a–c). The COX-2 can produce reactive oxygen species to stimulate intestinal macrophage activation, causing a high expression of NLRP3 in the colon [27]. In turn, the activated NLRP3 triggers the secretion of IL-1β and other inflammatory cytokines [28]. In addition, phosphorylation of JNK prompts the expression of *Il-1β* and *Il-6* in DSS-induced UC [29]. Overactivation of these cytokines will further exacerbate the abnormal immune responses in the colon [30]. Reversely, 5-ASA suppressed the above inflammatory responses in DSS-induced colitis. In addition, the interaction of 5-ASA with DSS has not been reported. Based on these findings, we propose that 5-ASA can exert a therapeutic effect on colitis by suppressing colonic inflammatory infiltration and inflammasome activation.

The gut barrier consists of epithelial tight junctions and a protective mucus layer produced by goblet cells [31]. The tight-junction protein ZO-1 maintains intestinal

epithelial integrity, while numerous mucins synthesized by colonic goblet cells constitute the thick mucus barrier [32]. Colons with impaired epithelial barrier are often accompanied by intestinal crypt infection and mucin secretion reduction, producing inflammatory reactions caused by harmful bacteria [33]. In this study, 5-ASA increased the expression of *Zo-1* and mucins in DSS-treated mice, indicating the protective effect of 5-ASA on the damage to gut barrier integrity and mucus barrier (Fig. 1f–h, 2e–f and Supplementary Fig. 1c). An in vitro research validated that JNK mediated the degradation of ZO-1 in jejunal IPEC-J2 cells [34]. Hence, 5-ASA might protect the intestinal barrier by attenuating colonic JNK. Meanwhile, intestinal barrier dysfunction in inflammatory bowel diseases (IBD) results in diarrhea via a leak-flux mechanism, which acts through epithelial sodium channel (ENaC) and Aquaporins (AQPs) [35]. The ENaC family and AQPs are in charge of water reabsorption in the colon, and the hindrance of these factors leads to incomplete aqueous reabsorption and diarrhea formation [36]. Here, we demonstrated that 5-ASA up-regulated the mRNA levels of colonic ENaC and AQPs in DSS-treated mice (Fig. 2d and g), consistent with the improvement of 5-ASA on the DAI score (Fig. 1b). In conclusion, 5-ASA could suppress epithelial tight junction and mucus barrier damage, and fluid–electrolyte metabolism disorder in DSS-treated mice.

To explore the role of gut microbiota in treating colitis by 5-ASA, we compared the abundance alteration of intestinal flora in DSS-treated mice with or without 5-ASA administration. Though 5-ASA failed to affect the bacterial changes at phylum levels in DSS-induced colitis, it had a positive regulatory effect on various bacteria at family and genus levels (Fig. 3d, e, Supplementary Fig. 2d). Especially, 5-ASA reduced the abundances of some harmful genera like *Desulfovibrio* and *Alloprevotella*, and raised the contents of several beneficial genera such as *Lachnospiraceae* and *Bifidobacterium* (Fig. 3e). *Desulfovibrio* is the main sulfate-reducing and H₂S-generating bacteria in the human colonic microbiota. The rich sulfate groups of DSS (17%) provide sufficient substrates to boost *Desulfovibrio* growth [37]. Breakage of intestinal epithelium caused by sulfate accumulation is a significant reason for DSS-induced UC [38]. Hence, the suppression of 5-ASA on *Desulfovibrio* sheds light on its therapeutic mechanism (Fig. 3d). *Alloprevotella* is a cancer-associated bacterium, which deteriorates the intestinal lining during UC occurrence [39]. Conversely, the *Lachnospiraceae* genus, belonging to the *Lachnospiraceae* family, was negatively associated with UC severity [39]. *Lachnospiraceae* is a butyric acid producer, protecting against human colon cancer [40]. Similarly, *Bifidobacterium* is another bacterium responsible for producing SCFAs with anti-inflammatory properties in the intestinal tract [41, 42]. The promotive effect of 5-ASA on *Bifidobacterium*

and *Lachnospiraceae* may contribute to its inhibition of colonic inflammation. Some of these bacterial changes, such as the increased abundance of *Bifidobacterium* and the attenuated trend of *Escherichia-Shigella*, were also observed in UC patients after 5-ASA treatment [21].

Among three primary intestinal metabolites in the colon of DSS-treated mice, 5-ASA did not affect the production of SCFAs, implying that SCFAs and their downstream signals were not involved in the rescue of colitis by 5-ASA (Fig. 5d). However, 5-ASA statistically increased the indole content in DSS-treated mice (Fig. 5e). Indole is a tryptophan catabolite that can inhibit quorum sensing and block virulence factors in non-indole-producing bacteria [43]. The increment of fecal indole by 5-ASA should be beneficial for colitis recovery. Noticeably, BAs were the most changed metabolites in colitis mice with 5-ASA treatment (Fig. 5a–c). Intestinal bacteria mainly influence the colonic BAs with bile salt hydrolase (BSH) and 7 α -dehydroxylation activities [5, 44]. BSH is in charge of deconjugation, and previous studies reported the BSH activity in *Bacteroides* and *Bifidobacterium* [44, 45]. The 7 α -dehydroxylation reaction is necessary to convert primary BAs to secondary BAs [46, 47]. The enzymes involved in 7 α -dehydroxylation are encoded by bile acid-inducible genes, which were previously identified in *Romboutsia* [48]. Recently, metagenome-screening research shows that *Lachnospiraceae* and *Ruminococcaceae* are the main bacteria that express enzymes with 7 α -dehydroxylation activity [48]. 5-ASA elevated the *Romboutsia*, some *Ruminococcaceae* family members (*Anaerotruncus*, *Ruminococcaceae* UCG-005, and *Ruminococcaceae* UCG-004) and two *Lachnospiraceae* family members (*Roseburia* and *Lachnospiraceae*) in DSS-treated mice (Fig. 3e). Besides, *Bacteroides* belonging to the *Bacteroidaceae* family can also promote the transformation of primary BAs to secondary BAs by 7 α -dehydroxylation [44]. These bacteria contribute to the increased production of secondary BAs (UDCA and TUDCA) after 5-ASA administration (Fig. 5c). As for the individual BAs, UDCA has been clinically used to prevent colitis complications and experimentally used to inhibit colitis in mice [49, 50]. TUDCA was antagonistic to intestinal inflammation and displayed an inhibitory effect on experimental colitis [51, 52]. A high level of CA promoted the proliferation of abnormal intestinal crypts and the over-expression of colon carcinogenic genes [53, 54]. Interestingly, in a report, the researchers used a UDCA-5-ASA conjugate to prevent colon carcinogenesis in rats [55]. It is thus possible that 5-ASA alleviated colitis symptoms in mice by regulating the bacterial transformation of BAs.

BA receptors (like FXR and TGR5)-mediated signaling pathways affect the BA metabolism and systemic inflammation in hosts. Among them, FXR governs the synthesis, secretion, and reabsorption of BAs in the liver and gut [56]. On the one hand, the hepatic FXR/SHP (Small heterodimer

partner) signaling controls the expressions of *Cyp7a1* and *Cyp8b1* by negative feedback regulation. On the other hand, the activation of intestinal FXR will promote the secretion of FGF15 (fibroblast growth factor 15). After FGF15 enters the blood, it binds to FGFR4 to inhibit the expressions of *Cyp7a1* and *Cyp8b1* [57, 58]. In parallel, our studies show that DSS treatment reduced FXR and FGFR4 expressions, which promoted BA synthetic enzymes' transcriptions (*Cyp7a1*, *Cyp8b1*, and *Cyp27a1*) and subsequent production of total BAs in mice (Figs. 5, 6, and 7). On the contrary, 5-ASA decreased the content of fecal BAs in DSS-treated mice by repressing the transcriptions of bile acid synthetic enzymes. Besides FXR, the hepatic TGR5 activation can trigger inflammatory responses by phosphorylating the ERK signaling [44]. Thus, the attenuated protein levels of hepatic TGR5 and p-ERK by 5-ASA should be helpful in relieving systemic inflammation in DSS-treated mice (Fig. 7c and d). Although, the enhanced TGR5 expression was beneficial for the regeneration of intestinal epithelial cells [59]. However, the alteration of TGR5 in colon tissue was not significant after 5-ASA treatment (Fig. 6b). These data support the notion that 5-ASA affected the contents of fecal BAs by regulating the FXR and TGR5 signaling pathways in DSS-treated mice. In a clinical study, IBD was accompanied by a decreased level of ASBT [60], implying that 5-ASA may reduce the fecal bile acid levels of DSS-treated mice by increasing ASBT expression and then promoting ASBT-dependent BA reabsorption. However, our result shows that 5-ASA elevated the mRNA and protein levels of ASBT in conventional colitis mice (Fig. 6a and b), not the gut microbiota-depleted colitis mice (Fig. 9a and b). This proved that the down-regulated effect of 5-ASA on intestinal bile acids should be initiated through its regulation of gut microbiota. Then, Spearman's correlation analysis revealed that these bile acid metabolism-related regulators correlated with the most altered bacterial genera in DSS-treated mice (Supplementary Fig. 3).

In a previous study, the authors found the regulation of 5-ASA on gut microbiota in UC patients, but they did not verify the role of intestinal flora in UC treatment [21]. In this study, we further proved the necessity of gut microbiota in the therapeutic effect of 5-ASA on colitis by conducting a germ-depletion experiment (Figs. 8 and 9). Noticeably, the inflammatory responses in colon tissues of DSS-treated mice were not suppressed by the antibiotic mixture (Fig. 8), suggesting that the DSS-induced colitis model should be convincible in the antibiotic-treated mice. In addition, 5-ASA failed to reverse the over-expression of pro-inflammatory factors in DSS-treat mice with germ-depleted (Fig. 8f), proving that 5-ASA had no direct anti-inflammatory effect on mouse colitis. We presume that 5-ASA may initiate an

indirect therapeutic effect on colitis through two pathways: (1) 5-ASA affected the abundances or metabolic activities of gut microbiota, which then led to the changes of intestinal metabolites like bile acids and indole; (2) 5-ASA was metabolized to new products (like *N*-acetyl-5-ASA) by intestinal bacteria. Next, bile acids, indole, *N*-acetayl-5-ASA, and other intestinal metabolites displayed anti-inflammatory or additional pharmacological effects on colitis. For instance, 5-ASA was metabolized by gut microbiota mainly colonized in the colonic tract after the administration [61]. In a previous report, the mucosal concentration of *N*-acetyl-5-ASA was related to endoscopic activity in ulcerative colitis patients [62]. As expected, 5-ASA showed no regulatory effect on the changes of bile acid metabolism indicators in DSS-induced colitis mice with germ depletion (Fig. 9 and Supplementary Fig. 6). From the above, we elucidated that reshaping the disordered gut microbiota community should benefit the BA metabolism and subsequent colitis alleviation.

In summary, our studies documented that 5-ASA improved colitis symptoms in DSS-treated mice, such as increased body weight gain and colon length, decreased DAI score and spleen index, and ameliorated gut barrier damage. The underlying molecular mechanisms of 5-ASA include: (1) reshaping of imbalanced gut microbiota structure; (2) restoring of bile acid metabolism; (3) mitigation of colonic inflammation. These findings provide new theoretical evidence for the clinical application of 5-ASA in colitis treatment.

Supplementary Information The online version contains supplementary material available at <https://doi.org/10.1007/s00018-022-04471-3>.

Author contributions HTL and AZL designed the study; LH, JPZ, GJS, HBY, XJS, and XWY performed the experiments and collected the data; LH and HTL analyzed the data; and LH and JPZ wrote the paper.

Funding The study was supported by Department of Science and Technology of Hubei Province (No. 2020CFB526 and No. 2021CFA014), Hubei Province Health Committee (No. ZY2021Z005, No. ZY2021M015, and No. ZY2021Q034), National Natural Science Foundation of China (No. 81873098), and Project of Hubei Hospital of Traditional Chinese Medicine (No. 2021YJKT-16).

Data availability statement The data that support the findings of this study are available from the corresponding author upon reasonable request. Raw data of 16S rDNA sequencing were shared on the about gut microbiota on NCBI Sequence Read Archive (SRA, <https://www.ncbi.nlm.nih.gov/sra>) with the record number PRJNA803597. Some data may not be made available because of privacy or ethical restrictions.

Declarations

Conflict of interest The authors declare that they have no conflict of interest.

Ethical approval All animal experimental procedures were performed in accordance with the Ethical Experimentation Committee of Hubei University of Chinese Medicine and the National Act on Use of Experimental Animals (Permission ID: SYXK2020-0002).

References

- Kaplan GG (2015) The global burden of IBD: from 2015 to 2025. *Nat Rev Gastroenterol Hepatol* 12:720–727. <https://doi.org/10.1038/nrgastro.2015.150>
- Maennich D, Marshall L (2020) Ulcerative colitis. *Nat Rev Dis Primers* 6:73. <https://doi.org/10.1038/s41572-020-00215-4>
- Ungaro R, Mehandru S, Allen PB, Peyrin-Biroulet L, Colombel JF (2017) Ulcerative colitis. *Lancet* 389:1756–1770. [https://doi.org/10.1016/S0140-6736\(16\)32126-2](https://doi.org/10.1016/S0140-6736(16)32126-2)
- Marchesi JR, Adams DH, Fava F, Hermes GD, Hirschfield GM, Hold G, Quraishi MN, Kinross J, Smidt H, Tuohy KM, Thomas LV, Zoetendal EG, Hart A (2016) The gut microbiota and host health: a new clinical frontier. *Gut* 65:330–339. <https://doi.org/10.1136/gutjnl-2015-309990>
- Sinha SR, Haileselassie Y, Nguyen LP, Tropini C, Wang M, Becker LS, Sim D, Jarr K, Spear ET, Singh G, Namkoong H, Bittinger K, Fischbach MA, Sonnenburg JL, Habtezion A (2020) Dysbiosis-induced secondary bile acid deficiency promotes intestinal inflammation. *Cell Host Microbe* 27(659–70):e5. <https://doi.org/10.1016/j.chom.2020.01.021>
- Costello SP, Hughes PA, Waters O, Bryant RV, Vincent AD, Blatchford P, Katsikeros R, Makanyanga J, Campaniello MA, Mavrangelos C, Rosewarne CP, Bickley C, Peters C, Schoeman MN, Conlon MA, Roberts-Thomson IC, Andrews JM (2019) Effect of fecal microbiota transplantation on 8-week remission in patients with ulcerative colitis: a randomized clinical trial. *JAMA* 321:156–164. <https://doi.org/10.1001/jama.2018.20046>
- Michaudel C, Sokol H (2020) The gut microbiota at the service of immunometabolism. *Cell Metab* 32:514–523. <https://doi.org/10.1016/j.cmet.2020.09.004>
- Wahlstrom A, Sayin SI, Marschall HU, Backhed F (2016) Intestinal crosstalk between bile acids and microbiota and its impact on host metabolism. *Cell Metab* 24:41–50. <https://doi.org/10.1016/j.cmet.2016.05.005>
- Jahnel J, Fickert P, Hauer AC, Hogenauer C, Avian A, Trauner M (2014) Inflammatory bowel disease alters intestinal bile acid transporter expression. *Drug Metab Dispos* 42:1423–1431. <https://doi.org/10.1124/dmd.114.058065>
- Gruner N, Mattner J (2021) Bile acids and microbiota: multifaceted and versatile regulators of the liver-gut axis. *Int J Mol Sci* 22:1397. <https://doi.org/10.3390/ijms22031397>
- Liu P, Wang Y, Yang G, Zhang Q, Meng L, Xin Y, Jiang X (2021) The role of short-chain fatty acids in intestinal barrier function, inflammation, oxidative stress, and colonic carcinogenesis. *Pharmacol Res* 165:105420. <https://doi.org/10.1016/j.phrs.2021.105420>
- Parada Venegas D, De la Fuente MK, Landskron G, Gonzalez MJ, Quera R, Dijkstra G, Harmsen HJM, Faber KN, Hermoso MA (2019) Short Chain Fatty Acids (SCFAs)-mediated gut epithelial and immune regulation and its relevance for inflammatory bowel diseases. *Front Immunol* 10:277. <https://doi.org/10.3389/fimmu.2019.00277>
- Nikolaus S, Schulte B, Al-Massad N, Thieme F, Schulte DM, Bethge J, Rehman A, Tran F, Aden K, Hasler R, Moll N, Schutze G, Schwarz MJ, Waetzig GH, Rosenstiel P, Krawczak M, Szymczak S, Schreiber S (2017) Increased tryptophan metabolism is associated with activity of inflammatory bowel diseases. *Gastroenterology* 153(1504–16):e2. <https://doi.org/10.1053/j.gastro.2017.08.028>
- Rubin DT, Ananthakrishnan AN, Siegel CA, Sauer BG, Long MD (2019) ACG clinical guideline: ulcerative colitis in adults. *Am J Gastroenterol* 114:384–413. <https://doi.org/10.14309/ajg.000000000000152>
- Podolsky DK (2002) Inflammatory bowel disease. *N Engl J Med* 347:417–429. <https://doi.org/10.1056/NEJMra020831>
- Lopez-Alarcon C, Rocco C, Lissi E, Carrasco C, Squella JA, Nunez-Vergara L, Speisky H (2005) Reaction of 5-aminosalicylic acid with peroxy radicals: protection and recovery by ascorbic acid and amino acids. *Pharm Res* 22:1642–1648. <https://doi.org/10.1007/s11095-005-6948-y>
- Jiang GL, Im WB, Donde Y, Wheeler LA (2010) Comparison of prostaglandin E2 receptor subtype 4 agonist and sulfasalazine in mouse colitis prevention and treatment. *J Pharmacol Exp Ther* 335:546–552. <https://doi.org/10.1124/jpet.110.173252>
- Cevallos SA, Lee JY, Velazquez EM, Foegeding NJ, Shelton CD, Tiffany CR, Parry BH, Stull-Lane AR, Olsan EE, Savage HP, Nguyen H, Ghanaat SS, Byndloss AJ, Agu IO, Tsoilis RM, Byndloss MX, Baumler AJ (2021) 5-Aminosalicylic acid ameliorates colitis and checks dysbiotic *Escherichia coli* expansion by activating PPAR- γ signaling in the intestinal epithelium. *MBio* 12:e03227-20. <https://doi.org/10.1128/mBio.03227-20>
- Jeong S, Lee H, Kim S, Ju S, Kim W, Cho H, Kim HY, Heo G, Im E, Yoo JW, Yoon IS, Jung Y (2020) 5-Aminosalicylic acid azo-coupled with a GPR109A agonist is a colon-targeted anticolic drug with a reduced risk of skin toxicity. *Mol Pharm* 17:167–179. <https://doi.org/10.1021/acs.molpharmaceut.9b00872>
- Merlen G, Kahale N, Ursic-Bedoya J, Bidault-Jourdainne V, Simerabet H, Doignon I, Tanfin Z, Garcin I, Pean N, Gautherot J, Davit-Spraul A, Guettier C, Humbert L, Rainteau D, Ebnet K, Ullmer C, Cassio D, Tordjmann T (2020) TGR5-dependent hepatoprotection through the regulation of biliary epithelium barrier function. *Gut* 69:146–157. <https://doi.org/10.1136/gutjnl-2018-316975>
- Xu J, Chen N, Wu Z, Song Y, Zhang Y, Wu N, Zhang F, Ren X, Liu Y (2018) 5-Aminosalicylic acid alters the gut bacterial microbiota in patients with ulcerative colitis. *Front Microbiol* 9:1274. <https://doi.org/10.3389/fmicb.2018.01274>
- Singh S, Feuerstein JD, Binion DG, Tremaine WJ (2019) AGA technical review on the management of mild-to-moderate ulcerative colitis. *Gastroenterology* 156(769–808):e29. <https://doi.org/10.1053/j.gastro.2018.12.008>
- He R, Li Y, Han C, Lin R, Qian W, Hou X (2019) L-Fucose ameliorates DSS-induced acute colitis via inhibiting macrophage M1 polarization and inhibiting NLRP3 inflammasome and NF- κ B activation. *Int Immunopharmacol* 73:379–388. <https://doi.org/10.1016/j.intimp.2019.05.013>
- Bauer C, Duewell P, Mayer C, Lehr HA, Fitzgerald KA, Dauer M, Tschopp J, Endres S, Latz E, Schnurr M (2010) Colitis induced in mice with dextran sulfate sodium (DSS) is mediated by the NLRP3 inflammasome. *Gut* 59:1192–1199. <https://doi.org/10.1136/gut.2009.197822>
- Hardin JA, Wallace LE, Wong JF, O'Loughlin EV, Urbanski SJ, Gall DG, MacNaughton WK, Beck PL (2004) Aquaporin expression is downregulated in a murine model of colitis and in patients with ulcerative colitis, Crohn's disease and infectious colitis. *Cell Tissue Res* 318:313–323. <https://doi.org/10.1007/s00441-004-0932-4>
- Kobayashi T, Siegmund B, Le Berre C, Wei SC, Ferrante M, Shen B, Bernstein CN, Danese S, Peyrin-Biroulet L, Hibi T (2020) Ulcerative colitis. *Nat Rev Dis Primers* 6:74. <https://doi.org/10.1038/s41572-020-0205-x>
- Deng Z, Ni J, Wu X, Wei H, Peng J (2020) GPA peptide inhibits NLRP3 inflammasome activation to ameliorate colitis through

- AMPK pathway. *Aging* (Albany NY) 12:18522–18544. <https://doi.org/10.18632/aging.103825>
28. Castro-Dopico T, Dennison TW, Ferdinand JR, Mathews RJ, Fleming A, Clift D, Stewart BJ, Jing C, Strongili K, Labzin LI, Monk EJM, Saeb-Parsy K, Bryant CE, Clare S, Parkes M, Clatworthy MR (2019) Anti-commensal IgG drives intestinal inflammation and type 17 immunity in ulcerative colitis. *Immunity* 50:1099–1114. <https://doi.org/10.1016/j.immuni.2019.02.006> (e10)
 29. Hou S, Yang X, Tong Y, Yang Y, Chen Q, Wan B, Wei R, Wang Y, Zhang Y, Kong B, Huang J, Chen Y, Lu T, Hu Q, Du D (2021) Structure-based discovery of 1*H*-indole-2-carboxamide derivatives as potent ASK1 inhibitors for potential treatment of ulcerative colitis. *Eur J Med Chem* 211:113114. <https://doi.org/10.1016/j.ejmech.2020.113114>
 30. Luo S, Wen R, Wang Q, Zhao Z, Nong F, Fu Y, Huang S, Chen J, Zhou L, Luo X (2019) Rhubarb Peony Decoction ameliorates ulcerative colitis in mice by regulating gut microbiota to restoring Th17/Treg balance. *J Ethnopharmacol* 231:39–49. <https://doi.org/10.1016/j.jep.2018.08.033>
 31. Parikh K, Antanaviciute A, Fawcner-Corbett D, Jagielowicz M, Aulicino A, Lagerholm C, Davis S, Kinchen J, Chen HH, Alham NK, Ashley N, Johnson E, Hublitz P, Bao L, Lukomska J, Andev RS, Bjorklund E, Kessler BM, Fischer R, Goldin R, Koohy H, Simmons A (2019) Colonic epithelial cell diversity in health and inflammatory bowel disease. *Nature* 567:49–55. <https://doi.org/10.1038/s41586-019-0992-y>
 32. van der Post S, Jabbar KS, Birchenough G, Arike L, Akhtar N, Sjoval H, Johansson MEV, Hansson GC (2019) Structural weakening of the colonic mucus barrier is an early event in ulcerative colitis pathogenesis. *Gut* 68:2142–2151. <https://doi.org/10.1136/gutjnl-2018-317571>
 33. Ahlawat S, Kumar P, Mohan H, Goyal S, Sharma KK (2021) Inflammatory bowel disease: tri-directional relationship between microbiota, immune system and intestinal epithelium. *Crit Rev Microbiol* 47:254–273. <https://doi.org/10.1080/1040841X.2021.1876631>
 34. Li E, Horn N, Ajuwon KM (2021) Mechanisms of deoxynivalenol-induced endocytosis and degradation of tight junction proteins in jejunal IPEC-J2 cells involve selective activation of the MAPK pathways. *Arch Toxicol* 95:2065–2079. <https://doi.org/10.1007/s00204-021-03044-w>
 35. Anbazhagan AN, Priyamvada S, Alrefai WA, Dudeja PK (2018) Pathophysiology of IBD associated diarrhea. *Tissue Barriers* 6:e1463897. <https://doi.org/10.1080/21688370.2018.1463897>
 36. Zhang W, Xu Y, Chen Z, Xu Z, Xu H (2011) Knockdown of aquaporin 3 is involved in intestinal barrier integrity impairment. *FEBS Lett* 585:3113–3119. <https://doi.org/10.1016/j.febslet.2011.08.045>
 37. Dzierzewicz Z, Cwalina B, Weglarz L, Wisniowska B, Szczerba J (2004) Susceptibility of *Desulfovibrio desulfuricans* intestinal strains to sulfasalazine and its biotransformation products. *Med Sci Monit* 10:BR185-90
 38. Rowan F, Docherty NG, Murphy M, Murphy B, Calvin Coffey J, O'Connell PR (2010) *Desulfovibrio* bacterial species are increased in ulcerative colitis. *Dis Colon Rectum* 53:1530–1536. <https://doi.org/10.1007/DCR.0b013e3181f1e620>
 39. Wang CS, Li WB, Wang HY, Ma YM, Zhao XH, Yang H, Qian JM, Li JN (2018) VSL#3 can prevent ulcerative colitis-associated carcinogenesis in mice. *World J Gastroenterol* 24:4254–4262. <https://doi.org/10.3748/wjg.v24.i37.4254>
 40. Meehan CJ, Beiko RG (2014) A phylogenomic view of ecological specialization in the *Lachnospiraceae*, a family of digestive tract-associated bacteria. *Genome Biol Evol* 6:703–713. <https://doi.org/10.1093/gbe/evu050>
 41. Jakubczyk D, Leszczynska K, Gorska S (2020) The effectiveness of probiotics in the treatment of inflammatory bowel disease (IBD)—a critical review. *Nutrients* 12:1973. <https://doi.org/10.3390/nu12071973>
 42. Lee J, d'Aigle J, Atadja L, Quaicoe V, Honarpisheh P, Ganesh BP, Hassan A, Graf J, Petrosino J, Putluri N, Zhu L, Durgan DJ, Bryan RM Jr, McCullough LD, Venna VR (2020) Gut microbiota-derived short-chain fatty acids promote poststroke recovery in aged mice. *Circ Res* 127:453–465. <https://doi.org/10.1161/CIRCRESAHA.119.316448>
 43. Lee JH, Wood TK, Lee J (2015) Roles of indole as an interspecies and interkingdom signaling molecule. *Trends Microbiol* 23:707–718. <https://doi.org/10.1016/j.tim.2015.08.001>
 44. Jia W, Xie G, Jia W (2018) Bile acid-microbiota crosstalk in gastrointestinal inflammation and carcinogenesis. *Nat Rev Gastroenterol Hepatol* 15:111–128. <https://doi.org/10.1038/nrgastro.2017.119>
 45. Wang Y, Gao X, Zhang X, Xiao F, Hu H, Li X, Dong F, Sun M, Xiao Y, Ge T, Li D, Yu G, Liu Z, Zhang T (2021) Microbial and metabolic features associated with outcome of infliximab therapy in pediatric Crohn's disease. *Gut Microbes* 13:1–18. <https://doi.org/10.1080/19490976.2020.1865708>
 46. Mullish BH, McDonald JAK, Pechlivanis A, Allegretti JR, Kao D, Barker GF, Kapila D, Petrof EO, Joyce SA, Gahan CGM, Glegola-Madejska I, Williams HRT, Holmes E, Clarke TB, Thursz MR, Marchesi JR (2019) Microbial bile salt hydrolases mediate the efficacy of faecal microbiota transplant in the treatment of recurrent *Clostridioides difficile* infection. *Gut* 68:1791–1800. <https://doi.org/10.1136/gutjnl-2018-317842>
 47. Ridlon JM, Alves JM, Hylemon PB, Bajaj JS (2013) Cirrhosis, bile acids and gut microbiota: unraveling a complex relationship. *Gut Microbes* 4:382–387. <https://doi.org/10.4161/gmic.25723>
 48. Vital M, Rud T, Rath S, Pieper DH, Schluter D (2019) Diversity of Bacteria Exhibiting Bile Acid-inducible α -dehydroxylation Genes in the Human Gut. *Comput Struct Biotechnol J* 17:1016–1019. <https://doi.org/10.1016/j.csbj.2019.07.012>
 49. Rudolph G, Gotthardt DN, Kloeters-Plachky P, Kulaksiz H, Schirmacher P, Stiehl A (2011) In PSC with colitis treated with UDCA, most colonic carcinomas develop in the first years after the start of treatment. *Dig Dis Sci* 56:3624–3630. <https://doi.org/10.1007/s10620-011-1763-2>
 50. Van den Bossche L, Hindryckx P, Devisscher L, Devriese S, Van Welden S, Holvoet T, Vilchez-Vargas R, Vital M, Pieper DH, Vanden Bussche J, Vanhaecke L, Van de Wiele T, De Vos M, Laukens D (2017) Ursodeoxycholic acid and its taurine- or glycine-conjugated species reduce colitogenic dysbiosis and equally suppress experimental colitis in mice. *Appl Environ Microbiol* 83:e02766-16. <https://doi.org/10.1128/AEM.02766-16>
 51. Cao SS, Zimmermann EM, Chuang BM, Song B, Nwokoye A, Wilkinson JE, Eaton KA, Kaufman RJ (2013) The unfolded protein response and chemical chaperones reduce protein misfolding and colitis in mice. *Gastroenterology* 144:989–1000. <https://doi.org/10.1053/j.gastro.2013.01.023> (e6)
 52. Laukens D, Devisscher L, Van den Bossche L, Hindryckx P, Vandenbroucke RE, Vandewynckel YP, Cuvelier C, Brinkman BM, Libert C, Vandenabeele P, De Vos M (2014) Tauroursodeoxycholic acid inhibits experimental colitis by preventing early intestinal epithelial cell death. *Lab Invest* 94:1419–1430. <https://doi.org/10.1038/labinvest.2014.117>
 53. Hirose Y, Kuno T, Yamada Y, Sakata K, Katayama M, Yoshida K, Qiao Z, Hata K, Yoshimi N, Mori H (2003) Azoxymethane-induced beta-catenin-accumulated crypts in colonic mucosa of rodents as an intermediate biomarker for colon carcinogenesis. *Carcinogenesis* 24:107–121. <https://doi.org/10.1093/carcin/24.1.107>

54. Corpet DE, Tache S, Peiffer G (1997) Colon tumor promotion: is it a selective process? Effects of cholate, phytate, and food restriction in rats on proliferation and apoptosis in normal and aberrant crypts. *Cancer Lett* 114:135–138. [https://doi.org/10.1016/s0304-3835\(97\)04643-0](https://doi.org/10.1016/s0304-3835(97)04643-0)
55. Narisawa T, Fukaura Y, Takeba N, Nakai K (2002) Chemoprevention of N-methylnitrosourea-induced colon carcinogenesis by ursodeoxycholic acid-5-aminosalicylic acid conjugate in F344 rats. *Jpn J Cancer Res* 93:143–150. <https://doi.org/10.1111/j.1349-7006.2002.tb01252.x>
56. Chiang JY (2013) Bile acid metabolism and signaling. *Compr Physiol* 3:1191–1212. <https://doi.org/10.1002/cphy.c120023>
57. Di Ciaula A, Garruti G, Lunardi Baccetto R, Molina-Molina E, Bonfrate L, Wang DQH, Portincasa P (2017) Bile acid physiology. *Ann Hepatol* 16:S4–S14. <https://doi.org/10.5604/01.3001.0010.5493>
58. Perino A, Demagny H, Velazquez-Villegas L, Schoonjans K (2021) Molecular physiology of bile acid signaling in health, disease, and aging. *Physiol Rev* 101:683–731. <https://doi.org/10.1152/physrev.00049.2019>
59. Sorrentino G, Perino A, Yildiz E, El Alam G, Bou Sleiman M, Gioiello A, Pellicciari R, Schoonjans K (2020) Bile Acids Signal via TGR5 to Activate Intestinal Stem Cells and Epithelial Regeneration. *Gastroenterology* 159:956–968. <https://doi.org/10.1053/j.gastro.2020.05.067> (e8)
60. Fitzpatrick LR, Jenabzadeh P (2020) IBD and bile acid absorption: focus on pre-clinical and clinical observations. *Front Physiol* 11:564. <https://doi.org/10.3389/fphys.2020.00564>
61. Kim EK, Choi EJ (2015) Compromised MAPK signaling in human diseases: an update. *Arch Toxicol* 89:867–882. <https://doi.org/10.1007/s00204-015-1472-2>
62. Fukuda T, Naganuma M, Takabayashi K, Hagihara Y, Tanemoto S, Nomura E, Yoshimatsu Y, Sugimoto S, Nanki K, Mizuno S, Mikami Y, Fukuhara K, Sujino T, Mutaguchi M, Inoue N, Ogata H, Iwao Y, Abe T, Kanai T (2020) Mucosal concentrations of *N*-acetyl-5-aminosalicylic acid related to endoscopic activity in ulcerative colitis patients with mesalamine. *J Gastroenterol Hepatol* 35:1878–1885. <https://doi.org/10.1111/jgh.15059>

Publisher's Note Springer Nature remains neutral with regard to jurisdictional claims in published maps and institutional affiliations.